

# Association of OCT Angiography Parameters With Age in Cognitively Healthy Older Adults

Bryce W. Polascik, BS; Atalie C. Thompson, MD, MPH; Stephen P. Yoon, MD; James H. Powers, MD; James R. Burke, MD, PhD; Dilraj S. Grewal, MD; Sharon Fekrat, MD

**BACKGROUND AND OBJECTIVE:** To evaluate the association of changes in retinal anatomy and microvasculature with age and sex in cognitively healthy older adults.

**PATIENTS AND METHODS:** Cross-sectional study of cognitively healthy subjects aged 50 years and older who underwent optical coherence tomography angiography (OCTA) to estimate the association between age and sex with ganglion cell layer-inner plexiform layer (GC-IPL); central subfield thickness (CST); subfoveal choroidal thickness (CT); foveal avascular zone (FAZ) size; and superficial (SCP), deep (DCP), and whole capillary plexus (WCP) vessel density (VD) and perfusion density (PD) measured in the ETDRS 3-mm and 6-mm circle and rings.

**RESULTS:** Among 141 older adults (72.9% female; median age: 69 years), 282 eyes were imaged. Females had a greater CT, GC-IPL thickness, and FAZ size and a lower CST than males. After controlling for sex, both CT ( $P = .001$ ) and GC-IPL thickness ( $P < .001$ ) decreased with age, whereas FAZ size and CST did not. There was a reduction in VD and PD in SCP, DCP, and WCP with age in the 3-mm circle, 3-mm ring, and 6-mm circle (all  $P < .05$ ).

**CONCLUSIONS:** There is a significant reduction in both VD and PD, as well as decreased choroidal and GC-IPL thickness associated with aging, even beyond the fifth decade, in cognitively healthy adults.

[*Ophthalmic Surg Lasers Imaging Retina*. 2020;51:706-714.]

## INTRODUCTION

Decline in vision and cognition with healthy aging is a major public health concern as the aged population grows. Since the older population is often disproportionately affected by retinal pathology with an exponentially increased prevalence of age-related macular degeneration and glaucoma, it is important to recognize normal age-related retinal structural and microvasculature changes in older cognitively healthy adults in order to be able to detect true retinal microvascular pathology.<sup>1</sup>

Prior studies have reported variable findings regarding the impact of age on foveal avascular zone area and retinal microvasculature vessel (VD) and perfusion densities (PD).<sup>2-7</sup> One of the reasons for this variability is that quantitative values from the different optical coherence tomography angiography (OCTA) devices are not interchangeable since each device utilizes its own proprietary algorithm for flow detection and segmentation.<sup>8,9</sup> Measurements taken with the same machine and technique, however, are thought to be relatively consistent and reliable.<sup>9,10</sup> There remains a need for standardization of analytical methods and normative databases for each device and determination of age-related changes in the

From Duke University, Durham, North Carolina (BWP); the Department of Ophthalmology, Duke University Medical Center, Durham, North Carolina (ACT, DSG, SF); Duke University School of Medicine, Durham, North Carolina (JPY, JHP); and the Department of Neurology, Duke University Medical Center, Durham, North Carolina (JRB).

Originally submitted April 27, 2020. Revision received August 12, 2020. Accepted for publication November 9, 2020.

Presented in part as a poster at the American Academy of Ophthalmology Annual Meeting, October 27-30, 2018, Chicago, Illinois, and Duke Visible Thinking Undergraduate Research Symposium, April 22, 2019, Durham, North Carolina.

Supported in part by funding from Heed Ophthalmic Foundation (ACT), Duke Undergraduate Research Support Travel Grant (BWP).

The authors report no relevant financial disclosures.

Drs. Grewal and Fekrat contributed equally as senior authors on this paper. Address correspondence to Sharon Fekrat, MD, 2351 Erwin Road, Durham, NC 27705; email: Sharon.fekrat@duke.edu.

doi: 10.3928/23258160-20201202-05

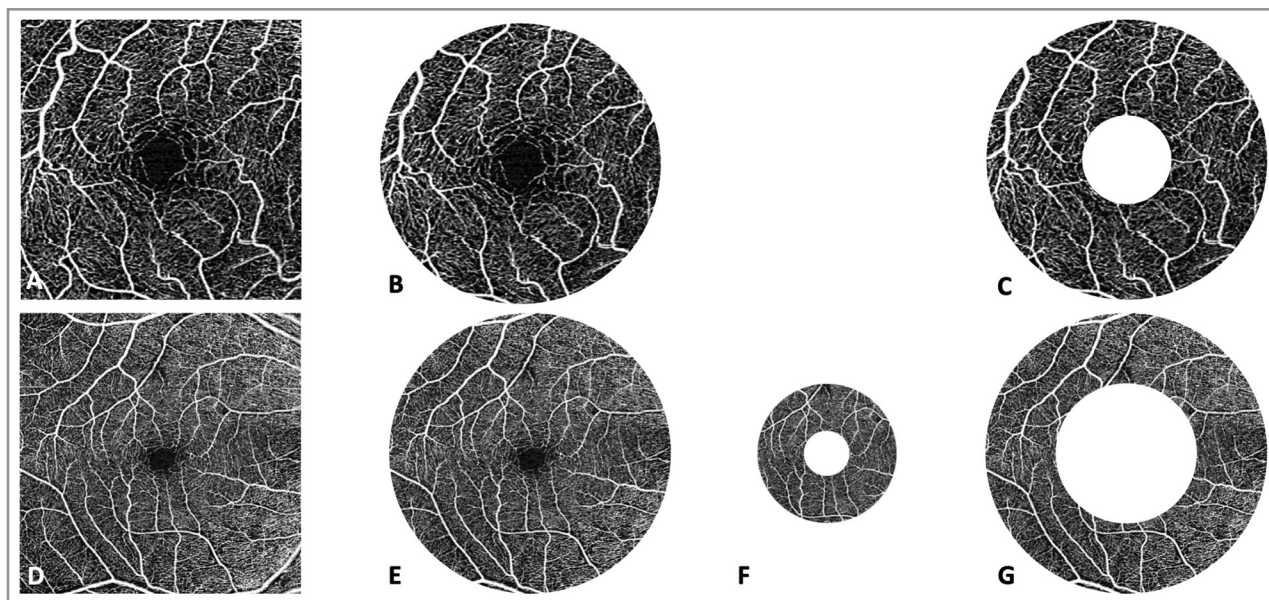


**Figure 1.** 3 mm × 3 mm (A) and 6 mm × 6 mm (D) optical coherence tomography angiography scans of the superficial capillary plexus with the different regions analyzed using the Early Treatment Diabetic Retinopathy Study grid sectors – the 3-mm circle (B), 3-mm ring (C), 6-mm circle (E), 6-mm inner ring (F), and 6-mm outer ring (G).

older population as prior studies have focused on mostly younger populations.

The goal of our study was to evaluate the relationship of age and sex on retinal structure and microvasculature in eyes of cognitively intact, healthy, older (> 50 years) adults in an effort to understand changes in these parameters with normal aging.

#### **PATIENTS AND METHODS**

This cross-sectional study was conducted at the Duke University Medical Center between July 2017 and June 2018 (Clinicaltrials.gov NCT03233646). Institutional review board approval was obtained through the Duke University School of Medicine in Durham, North Carolina. Written informed consent was obtained from all participants. The study adhered to the tenets of the Declaration of Helsinki.

Adult volunteers who were 50 years of age and older were recruited from relatives or attendants of patients from any Duke clinic, from the local community, or from the registry of control subjects in the Bryan Alzheimer's Disease Research Center (ADRC). On the day of enrollment, subjects underwent Mini-Mental State Examination (MMSE). Only eyes with corrected distance visual acuity (VA) of 20/40 or better using a standard Early Treatment Diabetic Retinopathy Study (ETDRS) chart were enrolled. Exclusion criteria included a known diagnosis of mild cognitive impairment, any dementia (including Alzheimer's disease, Parkinson's disease, among oth-

ers), neurological disease, stroke, diabetes mellitus, uncontrolled hypertension, any retinal disease including macular degeneration, optic nerve disease including glaucoma, refractive errors greater than +6.0 or -6.0 diopters (D), prior intraocular surgery other than cataract, inability to cooperate with testing, and other neurologic or age-related ocular conditions that may impact acquisition and segmentation of OCT and OCTA images.

#### **Optical Coherence Tomography and Optical Coherence Tomography Angiography Image Acquisition**

OCT and OCTA (Zeiss Cirrus HD-5000 Spectral-Domain OCT with AngioPlex, software version 10.0.0.14618; Carl Zeiss Meditec, Dublin, CA) images were obtained by trained imagers (BWP, SPY, ACT) for both eyes of each subject without pharmacologic pupillary dilation. Motion-tracking capabilities using an optical microangiography algorithm for analysis were used.<sup>11</sup> Images were excluded if they were deemed to be poor quality images, which was defined as a signal strength less than 7/10, presence of motion artifacts, low resolution or saturation, or poor centration. The OCT images obtained included the 512 × 128 macular cube and high definition 21-line with enhanced depth imaging (EDI). The 512 × 128 cube scan captures data in a 6-mm square grid by acquiring a series of 128 horizontal scan lines each composed of 512 A-scans using a 47-μm spacing between lines and 1,024 data points per A scan. The 21-line EDI scan

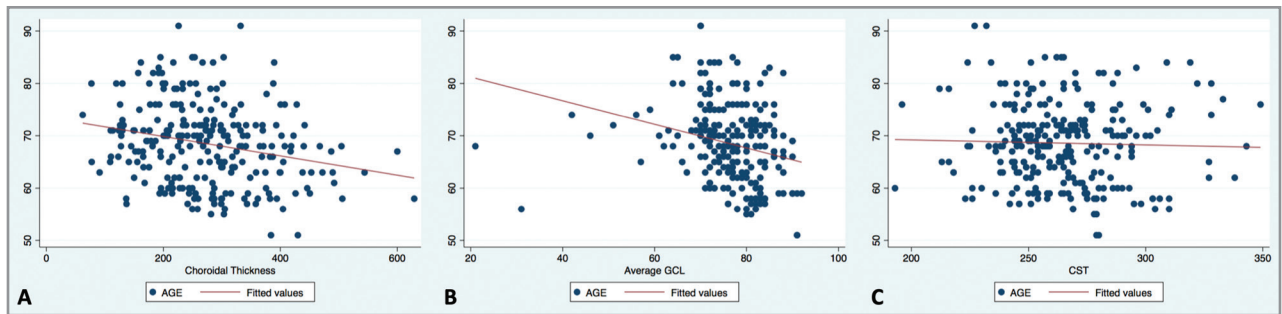


**Figure 2.** Scatterplots showing associations between age and choroidal thickness (A), average ganglion cell layer-inner plexiform layer (GC-IPL) thickness (B), and central subfield thickness (CST) (C).

captures 21 high-definition horizontal scan lines at a depth of 2.0 mm with eight acquired B-scans for each line, and each B-scan composed of 1,024 A-scans. The scan spacing was 0.3 mm between scans, and the scan length was 9 mm. The individual scans were reviewed to verify correct segmentation of the retinal layers and those with incorrect segmentation were excluded. The OCTA images were obtained using 3 mm × 3 mm and 6 mm × 6 mm OCTA scan patterns, both centered on the fovea.<sup>11</sup>

### Optical Coherence Tomography and Optical Coherence Tomography Angiography Image Analysis

Central subfield thickness (CST) was measured as the thickness between the inner limiting membrane and retinal pigment epithelium (RPE) at the fovea from the macular cube. Average ganglion cell layer-inner plexiform layer (GC-IPL) thickness was quantified within a 14.13 mm<sup>2</sup> elliptical annulus area centered on the fovea.<sup>12</sup>

Two trained graders (BWP, JHP) independently reviewed and graded the subfoveal choroidal thickness (CT) on the EDI images. The CT was drawn perpendicularly from the outer border of RPE to the inner border of the sclerochoroidal junction using the software's caliper tool.<sup>13-15</sup> Values with a difference greater than 5% were reviewed jointly by the graders, and a consensus value was determined. For values with less than 5% difference, final values were obtained by averaging the two measurements.

Full-thickness retinal scans were deconstructed into the superficial capillary plexus (SCP), deep capillary plexus (DCP), and whole capillary plexus (WCP). The inner boundary of the SCP slab was defined as the internal limiting membrane (ILM) and outer boundary was the inner plexiform layer. The inner boundary of the DCP slab was the inner plexiform layer and the outer boundary was the outer plexiform layer. Projection shadows were removed prior to analysis of the DCP. The WCP slab was defined from the ILM

to 70 μm above the RPE. The individual OCTA slabs were reviewed to check for errors in segmentation of the different capillary plexuses, and those with segmentation errors were excluded. The SCP FAZ boundaries were calculated by the software and were reviewed manually. Inaccurate boundaries identified on manual review (DSG) were corrected or excluded.

The software quantified the average VD and PD using an ETDRS grid overlay (Figure 1). VD was defined as the total length of perfused vasculature per unit area, whereas PD was defined as the total area of perfused vasculature per unit area. VD and PD were averaged over the 3-mm ETDRS circle and ring for 3 mm × 3 mm images and the 6-mm ETDRS circle and rings for 6 mm × 6 mm scans.

### Statistical Analysis

All statistical analyses were completed in STATA 15.1 (StataCorp, College Station, TX). ETDRS VAs were converted to the logarithm of the minimum angle of resolution (logMAR) scale. Descriptive statistics of the study subjects, demographic characteristics, OCT and OCTA parameters were assessed in the SCP, DCP, and WCP. Separate linear generalized estimating equations (GEE) were constructed with each OCT (ie, CST, GC-IPL, CT) or OCTA (ie, FAZ, 3-mm and 6-mm ETDRS circle and ring PD and VD) parameter serving as the dependent variable and either age or sex as the independent variable. An exchangeable correlation structure was set to account for when measurements were obtained on both eyes within a subject. When necessary, the dependent variable was transformed (eg, log, cubed) so as not to violate the assumption of normality. Finally, separate multivariate GEE models for each of the parameters were built with both age and sex adjusted for in the model. Since the nature of this analysis was exploratory and not confirmatory, P values presented are descriptive and exploratory in nature.

**TABLE 1**  
**Demographic Characteristics**

Variables	N = 133 Subjects (254 Eyes)
Age (Years)	
Mean ± Standard Deviation	69.2 ± 7.8
Median (Range)	69.8 (51, 91.2)
Sex – n (%)	
Female	97 (72.9%)
Male	36 (27.1%)
logMAR Corrected Visual Acuity	
Mean ± Standard Deviation	0.11 ± 0.1 (20/25)
Median (Range)	0.1 (0, 0.3)
	20/25 (20/20, 20/40)
Race	
White	110 (82.7%)
Asian	0
Black or African American	5 (3.8%)
American Indian or Alaska Native	0
Native Hawaiian or Other Pacific Islander	0
Hispanic or Latino	0
Other/Not Reported	18 (13.5%)
Mini-Mental State Examination Score	29.2 ± 1.1
Mean ± Standard Deviation	(Range: 25-30, Median: 30)

*logMAR = logarithm of the minimum angle of resolution*

## RESULTS

Two hundred and eighty-two eyes of 141 healthy older adults were imaged. Of the 282 eyes, images from 254 (90%) eyes of 133 adults were of sufficient quality to allow SCP image analysis. Twenty-eight eyes were excluded from SCP analysis due to poor OCTA image quality, motion artifact, inaccurate segmentation, or poor foveal centration. Good quality images of the DCP and WCP were available in 215 eyes of 112 subjects, with 39 eyes excluded due to uncorrectable projection artifact.

Table 1 shows the demographic characteristics of the 133 study subjects in our study population.

### OCT Parameters

The mean and median values of the OCT parameters are reported in Table 2A.

Supplemental Table 1 (available at [www.Healio.com/OSLIRetina](http://www.Healio.com/OSLIRetina)) displays the univariate GEE analysis for the association of either age or sex with each of the OCT parameters. For each year of increasing age, there was a significant decline in CT (Figure 2A)

(–2.99;  $P = .003$ ) and GC-IPL thickness (Figure 2B) (–5059;  $P < .001$ ). Age was associated with these parameters after adjusting for sex in multivariate analysis (Table 2b). CST (Figure 2C) was not associated with age (all  $P > .05$ ).

Female sex was associated with an increased CT (40.5;  $P = .018$ ) and GC-IPL thickness (46,992;  $P = .043$ ), but decreased CST (–18.4;  $P < .001$ ). Females had a thinner CST (–18.8;  $P < .001$ ), even after controlling for age ( $P < .001$ ).

### Superficial Capillary Plexus

The mean and median values of the OCTA of the SCP parameters are reported in Table 3A. Table 3B displays the univariate and multivariate GEE analysis for the association of either age or sex with each of the OCTA 3 mm × 3 mm and 6 mm × 6 mm SCP parameters. The FAZ area was not associated with age in either univariate or multivariate analyses (all  $P > .05$ ). Females had a larger FAZ area (0.39;  $P < .001$ ), even after controlling for age (all  $P < .001$ ). Both VD and PD in both the 3-mm and 6-mm ETDRS circle and

**TABLE 2A**  
**OCT Parameters in Normal Eyes of Adults 50 Years of Age or Older**

	Mean ± Standard Deviation
	Median (Range)
Central subfield thickness (μm)	264.3 ± 24.6 264 (193-349)
Choroidal thickness (μm)	274.1 ± 97.7 265 (62-629)
GC-IPL thickness (μm)	77.2 ± 7.6 77.5 (31-92)

OCT = optical coherence tomography; GC-IPL = ganglion cell layer-inner plexiform layer

**TABLE 2B**  
**Generalized Estimating Equations of the Multivariate Association Between Age or Sex and OCT Parameters**

	Age (Years)	Sex (F vs. M)
	Beta Coefficient (95% CI), P Value	Beta Coefficient (95% CI), P Value
Central subfield thickness (μm)	-0.23 (-0.72 to 0.26); P = .36	-18.8 (-27.2 to -10.4); P < .001
Choroidal thickness (μm)	-2.8 (-4.7 to -0.86); P = .005	35.4 (2.4-68.5); P = .036
GC-IPL thickness <sup>a</sup> (μm)	-4,819 (-7,289 to -2,350); P < .001	37,863 (-4,744 to 80,470); P = .082

Dependent variable underwent <sup>a</sup>cubic transformation.

OCT = optical coherence tomography; GC-IPL, ganglion cell layer-inner plexiform layer; F = female; M = male; CI = confidence interval

rings were similar among males and females (all  $P > .05$ ). Age was associated with VD and PD in the 3 mm × 3 mm circle and ring after adjusting for sex in multivariate analysis (all  $P < .001$ ); age was not associated with the VD and PD in the 6 mm × 6 mm circle or rings and was only associated with PD in the 6-mm circle after adjusting for sex in multivariate analysis ( $P = .025$ ) (Table 4B).

### Deep Capillary Plexus

The mean and median values of the OCTA DCP parameters are reported in Table 3a. Table 3b displays the univariate and multivariate GEE analysis for the association of either age or sex with each of the OCTA DCP parameters. Female sex was associated with decreased PD in the 3-mm circle ( $-0.0147$ ;  $P = .035$ ), VD in the 3-mm circle ( $-0.92$ ;  $P = .027$ ), and VD in the 3-mm ring ( $-0.91$ ;  $P = .046$ ). After adjusting for age in multivariate analysis, sex was associated with VD in the 3-mm circle and 3-mm ring (all  $P < .05$ ). Sex was not associated with PD or VD in the 6-mm parameters.

For each year of increasing age, the following parameters significantly decreased: PD in 3-mm circle ( $-0.0014$ ;  $P < .001$ ), VD in 3-mm circle ( $-0.078$ ;  $P = .001$ ), PD in 3-mm ring ( $-0.002$ ;  $P < .001$ ), VD in 3-mm ring ( $-0.085$ ;  $P = .001$ ), PD in 6-mm circle ( $-0.002$ ;  $P < .001$ ), VD in 6-mm circle ( $-0.099$ ;  $P < .001$ ), PD in 6-mm inner ring ( $-0.0028$ ;  $P < .001$ ), VD in 6-mm inner ring ( $-0.11$ ;  $P < .001$ ), PD in 6-mm outer ring ( $-0.002$ ;  $P < .001$ ), and VD in 6-mm outer ring ( $-0.098$ ;  $P < .001$ ). Age was associated with all of these parameters after adjusting for sex in multivariate analysis (Table 3B).

### Whole Capillary Plexus

The mean and median values of the OCTA WCP parameters are reported in Table 3A. Table 3B displays the univariate GEE analysis for the association of either age or sex with each of the OCTA WCP parameters. Female sex was not significantly associated with any of the WCP parameters (all  $P > .1$ ) in the univariate or multivariate GEE models. Age was significantly associated with all of the OCTA

**TABLE 3A**  
**OCTA 3 mm × 3 mm and 6 mm × 6 mm Superficial, Deep, and Whole Capillary Plexus Parameters in Normal Eyes of Adults Aged 50 Years and Older**

	Superficial Capillary Plexus	Deep Capillary Plexus	Whole Capillary Plexus
	n=254 Eyes	n=215 Eyes	n=215 Eyes
	Mean ± Standard Deviation Median (range)		
Foveal Avascular Zone (FAZ) Area <sup>a</sup> (mm <sup>2</sup> )	0.25 ± 0.11; 0.24 (0.038, 0.68)		
Vessel Density (/mm) in 3-mm ETDRS Circle	20.2 ± 1.6; 20.4 (14.2, 23.3)	15.1 ± 2.2; 15.2 (7.2, 20.9)	22.9 ± 1.4; 23.2 (17.3, 25.6)
Perfusion Density in 3-mm ETDRS Circle	0.365 ± 0.026; (0.368 (0.272, 0.462))	0.286 ± 0.037; 0.289 (0.147, 0.377)	0.391 ± 0.022; 0.394 (0.309, 0.474)
Vessel Density (/mm) in 3-mm ETDRS Ring	21.3 ± 1.5; 21.5 (15.3, 24.2)	15.9 ± 2.4; 16.0 (6.3, 21.7)	21.9 ± 1.4; 22.1 (16.5, 24.4)
Perfusion Density in 3-mm ETDRS Ring	0.386 ± 0.025; 0.388 (0.295, 0.456)	0.302 ± 0.042; 0.306 (0.127, 0.398)	0.408 ± 0.022; 0.412 (0.325, 0.464)
Vessel Density (/mm) in 6-mm ETDRS Circle	17.9 ± 1.1; 18.1 (14.2, 20.2)	13.7 ± 2.76; 14.2 (4.0, 18.5)	18.9 ± 0.81; 19.1 (14.0, 20.1)
Perfusion Density in 6-mm ETDRS Circle	0.440 ± 0.026; 0.446 (0.34, 0.487)	0.296 ± 0.067; 0.307 (0.077, 0.413)	0.464 ± 0.020; 0.469 (0.332, 0.492)
Vessel Density (/mm) in 6-mm ETDRS Inner Ring	17.9 ± 1.5; 18.3 (11.5, 20.4)	12.5 ± 3.0; 13.0 (2.6, 17.9)	18.7 ± 1; 18.9 (13.3, 20.5)
Perfusion Density in 6-mm ETDRS Inner Ring	0.431 ± 0.037; 0.441 (0.266, 0.479)	0.269 ± 0.072; 0.282 (0.047, 0.403)	0.447 ± 0.028; 0.453 (0.305, 0.488)
Vessel Density (/mm) in 6-mm ETDRS Outer Ring	18.2 ± 1.0; 18.4 (14.6, 20.2)	14.2 ± 2.8; 14.5 (4.0, 18.9)	19.1 ± 0.79; 19.3 (14.4, 20.3)
Perfusion Density in 6-mm ETDRS Outer Ring	0.451 ± 0.025; 0.458 (0.351, 0.496)	0.306 ± 0.069; 0.314 (0.076, 0.424)	0.471 ± 0.019; 0.476 (0.341, 0.50)

<sup>a</sup>Dependent variable underwent logarithmic transformation.

OCTA = optical coherence tomography angiography; ETDRS = Early Treatment Diabetic Retinopathy Study

parameters after adjusting for sex in the multivariate analysis (Table 3B).

## DISCUSSION

We describe OCT and OCTA parameters acquired in healthy eyes of cognitively healthy adults 50 years or older and evaluate the relationship of these measurements to age and sex. In our relatively large study population of 254 eyes, we found that there is significant decline of VD and PD in the superficial, deep, and whole capillary plexuses as well as decreased choroidal thickness and GC-IPL thickness with age. We also found that females have an increased FAZ, GC-IPL thickness, and CT but a decreased CST, even after controlling for age. Unique to prior investigations, we analyzed a group of older adults and also

evaluated their cognitive status since cognitive impairment is recognized to be associated with microvascular loss.<sup>16</sup>

Differences in VD measurements among different OCTA platforms are well recognized.<sup>8,17</sup> However, the majority of prior studies evaluating OCTA parameters including vessel and perfusion densities in healthy eyes used other OCTA imaging platforms and have generally assessed much younger adult populations.<sup>4,7,8</sup> As imaging technology advances, the availability of normative values in individuals of different ages and sexes is paramount to our understanding of not only pathologic changes but also non-pathologic changes attributed to age, sex, and racial differences. Parameters from various imaging devices are not directly comparable, and even different versions of soft-

TABLE 3B

### Generalized Estimating Equations of the Univariate and Multivariate Association Between Age or Sex and OCTA Superficial, Deep, and Whole Capillary Plexuses Parameters in Normal Eyes of Adults Aged 50 Years and Older

Parameter	Superficial Capillary Plexus		Deep Capillary Plexus		Whole Capillary Plexus	
	Age Beta Coefficient (95% CI); P Value	Sex (F vs. M) Beta Coefficient (95% CI); P Value	Age Beta Coefficient (95% CI); P Value	Sex (F vs. M) Beta Coefficient (95% CI); P Value	Age Beta Coefficient (95% CI); P Value	Sex (F vs. M) Beta Coefficient (95% CI); P Value
Foveal Avascular Zone (FAZ) Area <sup>a</sup> (mm <sup>2</sup> )	0.006 (-0.004 to 0.015); P = .26	0.39 (0.22-0.55); P < .001*				
Perfusion Density in 3-mm ETDRS Circle	-0.0011 (-0.0016 to -0.0007); P < .001*	-0.002 (-0.01 to 0.007); P = .71	-0.0014 (-0.0021 to -0.0006); P < .001*	-0.0147 (-0.028 to -0.001); P = .035	-0.00094 (-0.0013 to -0.0005); P < .001*	-0.003 (-0.011 to 0.0047); P = .427
Vessel Density (/mm) in 3-mm ETDRS Circle	-0.07 (-0.10 to -0.05); P < .001*	0.07 (-0.44 to 0.59); P = .78	-0.078 (-0.12, to -0.034); P = .001*	-0.92 (-1.74 to -0.106); P = .027*	-0.0596 (-0.084 to -0.035); P < .001*	-0.154 (-0.644 to 0.337); P = .54
Perfusion Density in 3-mm ETDRS Ring	-0.0011 (-0.0015 to -0.0007); P < .001*	0.0029 (-0.005 to 0.011); P = .48	-0.002 (-0.003 to -0.001); P < .001*	-0.016 (-0.033 to 0.002); P = .074*	-0.0009 (-0.0013 to -0.0005); P < .001*	-0.0003 (-0.008 to 0.0077); P = .94
Vessel Density <sup>b</sup> (/mm) in 3-mm ETDRS Ring	-94.5 (-127.7 to -61.3); P < .001*	445.2 (-198.5 to 1,089); P = .18	-0.085 (-0.13 to -0.037); P = .001*	-0.91 (-1.81 to -0.017); P = .046*	-0.060 (-0.085 to -0.034); P < .001*	-0.015 (-0.517 to 0.487); P = .95
Perfusion Density <sup>b</sup> in 6-mm ETDRS Circle	-0.0003 (-0.0006 to -0.0001); P = .033*	-0.0018 (-0.0065 to 0.0030); P = .47	-0.002 (-0.004 to -0.001); P < .001*	0.0005 (-0.0229 to 0.024); P = .965	-0.0005 (-0.0009 to 0.00014); P = .008*	0.0006 (-0.006 to 0.008); P = .86
Vessel Density <sup>b</sup> (/mm) in 6-mm ETDRS Circle	-23.7 (-41.8 to -5.7); P = .01*	-103.6 (-422.9 to 215.6); P = .5	-0.099 (-0.15 to -0.049); P < .001*	0.009 (-0.959 to 0.979); P = .98	-0.017 (-0.032 to -0.002); P = .028*	0.091 (-0.188 to 0.37); P = .52
Perfusion Density <sup>b</sup> in 6-mm ETDRS Inner Ring	-0.0002 (-0.0006 to 0.0001); P = .17	-0.0007 (-0.0065 to -0.0052); P = .82	-0.0028 (-0.004 to -0.001); P < .001*	0.001 (-0.024 to 0.027); P = .921	-0.0005 (-0.001 to -0.00003); P = .039*	-0.0028 (-0.012 to 0.006); P = .54
Vessel Density <sup>b</sup> (/mm) in 6-mm ETDRS Inner Ring	-18 (-41 to 4.9); P = .12	-16.2 (-416 to 383.2); P = .94	-0.11 (-0.17 to -0.059); P < .001*	0.041 (-1.0 to 1.09); P = .94	-0.020 (-0.040 to -0.0009); P = .04*	0.014 (-0.345 to 0.374); P = .94
Perfusion Density <sup>b</sup> in 6-mm ETDRS Outer Ring	-0.0002 (-0.0005 to 0.0001); P = .15	-0.0014 (-0.0062 to 0.0034); P = .56	-0.002 (-0.003 to -0.001); P < .001*	0.0002 (-0.024 to 0.024); P = .986	-0.0005 (-0.0008 to -0.000098); P = .012*	0.0020 (-0.0046 to 0.0086); P = .55
Vessel Density <sup>b</sup> (/mm) in 6-mm ETDRS Outer Ring	-11.8 (-29.7 to 6.1); P = .20	-48 (-358.7 to 262.6); P = .76	-0.098 (-0.149 to -0.046); P < .001*	0.001 (-0.983 to 0.985); P = .998	-0.013 (-0.028 to 0.001); P = .069	0.15 (-0.11 to 0.42); P = .26

\*P value significant at < .05 in multivariate generalized estimating equations model

Dependent variable underwent <sup>a</sup>logarithmic or <sup>b</sup>cubic transformation.

OCTA = optical coherence tomography angiography; ETDRS = Early Treatment Diabetic Retinopathy Study; F=female, M=male

ware in a single imaging device might lead to different values, making results not directly comparable.<sup>8,9,18-21</sup>

In our study, females had a larger FAZ area even after controlling for age. Although some prior studies have shown no sex-related differences in FAZ area,<sup>3,4</sup> an increasing number have shown a larger FAZ in females.<sup>6,22-24</sup> This may be related to the lower CST in females. We did not observe an association of FAZ area with age after controlling for sex.<sup>2,3,25</sup> Both VD and PD in both the 3-mm and 6-mm ETDRS circle and rings were similar among males and females.

We found that the VD and PD in the SCP, DCP, and WCP decreased with age. The association of lower VD of the SCP and DCP with older age may be explained by the physiologic age-related loss in vascularity. Loss of retinal microvasculature in the macula with increasing age is well recognized, and the macular region outside the FAZ itself may be more susceptible to age-related vascular perfusion changes relative to other regions of the retina. In a large, population-based study, You et al.<sup>26</sup> reported that VD in the SCP and DCP decreased by 0.13% and 0.22%, respectively, every year after 50 years of age. Yu et al. reported that VD decreased at an annual rate of 0.4%.<sup>24</sup> You et al. reported 0.116% (South Korean population), whereas Gadde et al.<sup>27</sup> and Rao et al.<sup>28</sup> reported an annual decline of 0.2%. There are challenges in directly comparing our findings with that of other studies in the published literature due to differences in OCTA imaging platforms and much younger adult populations with different racial distributions. In addition, due to a lack of consensus on standards for vessel and perfusion density measurements, it is difficult to validate quantification data.

Our study has several limitations. First, we did not compare select findings with fluorescein angiography or indocyanine green angiography, which were not obtained. Second, we did not assess any possible effects attributable to diurnal variation. Third, we did not perform ocular biometry so we did not correct for image magnification error induced by axial length; however, we excluded eyes with refractive errors greater than +6.0 or -6.0 D, which has been shown to reduce the magnitude of differences due to axial length, particularly for VD.<sup>29</sup> Fourth, each imaging parameter was individually modeled, so adjustments were not made for multiple tests as this was an exploratory analysis. Fifth, this was a cross-sectional study and subjects were not followed longitudinally to assess microvascular changes over time with advancing age. Finally, we excluded uncontrolled hypertension but not individuals with treated hypertension, and hypertension can result in decreased vascular density.<sup>30</sup>

In conclusion, we found that in a large cohort of healthy eyes of cognitively healthy subjects 50 years of age and older, the vessel and perfusion densities in the superficial, deep, and whole capillary plexuses decrease with age, even beyond the fifth decade. These changes need to be considered when evaluating microvascular alterations in older adults in order to distinguish true retinal pathology from expected changes due to sex differences and normal aging. Future studies following such an older healthy cohort prospectively will allow determination of longitudinal changes in the retinal vascular plexuses with advancing age and in different sexes and racial groups, as well as comparison to other imaging devices.

## REFERENCES

1. Tielsch JM, Sommer A, Katz J, Royall RM, Quigley HA, Javitt J. Racial variations in the prevalence of primary open-angle glaucoma. The Baltimore Eye Survey. *JAMA*. 1991;266(3):369-374. <https://doi.org/10.1001/jama.1991.03470030069026> PMID:2056646
2. Wu LZ, Huang ZS, Wu DZ, Chan E. Characteristics of the capillary-free zone in the normal human macula. *Jpn J Ophthalmol*. 1985;29(4):406-411. PMID:3831489
3. Samara WA, Say EA, Khoo CT, et al. CORRELATION OF FOVEAL AVASCULAR ZONE SIZE WITH FOVEAL MORPHOLOGY IN NORMAL EYES USING OPTICAL COHERENCE TOMOGRAPHY ANGIOGRAPHY. *Retina*. 2015;35(11):2188-2195. <https://doi.org/10.1097/IAE.0000000000000847> PMID:26469536
4. Coscas F, Sellam A, Glacet-Bernard A, et al. Normative Data for Vascular Density in Superficial and Deep Capillary Plexuses of Healthy Adults Assessed by Optical Coherence Tomography Angiography. *Invest Ophthalmol Vis Sci*. 2016;57(9):OCT211-OCT223. <https://doi.org/10.1167/iovs.15-18793> PMID:27409475
5. Garrity ST, Iafe NA, Phasukkijwatana N, Chen X, Sarraf D. Quantitative Analysis of Three Distinct Retinal Capillary Plexuses in Healthy Eyes Using Optical Coherence Tomography Angiography. *Invest Ophthalmol Vis Sci*. 2017;58(12):5548-5555. <https://doi.org/10.1167/iovs.17-22036> PMID:29075766
6. Gómez-Ulla F, Cutrin P, Santos P, et al. Age and gender influence on foveal avascular zone in healthy eyes. *Exp Eye Res*. 2019;189:107856. <https://doi.org/10.1016/j.exer.2019.107856> PMID:31654619
7. Iafe NA, Phasukkijwatana N, Chen X, Sarraf D. Retinal Capillary Density and Foveal Avascular Zone Area Are Age-Dependent: Quantitative Analysis Using Optical Coherence Tomography Angiography. *Invest Ophthalmol Vis Sci*. 2016;57(13):5780-5787. <https://doi.org/10.1167/iovs.16-20045> PMID:27792812
8. Magrath GN, Say EAT, Sioufi K, Ferenczy S, Samara WA, Shields CL. VARIABILITY IN FOVEAL AVASCULAR ZONE AND CAPILLARY DENSITY USING OPTICAL COHERENCE TOMOGRAPHY ANGIOGRAPHY MACHINES IN HEALTHY EYES. *Retina*. 2017;37(11):2102-2111. <https://doi.org/10.1097/IAE.0000000000001458> PMID:27997512
9. Waheed NRC, Arya M, Alibhai Y, et al. Retinal vessel density: a comparison across optical coherence tomography angiography (OCTA) devices in healthy eyes. The Retina Society; 2017.
10. Lei J, Durbin MK, Shi Y, et al. Repeatability and Reproducibility of Superficial Macular Retinal Vessel Density Measurements Using Optical Coherence Tomography Angiography En Face Images. *JAMA Ophthalmol*. 2017;135(10):1092-1098. <https://doi.org/10.1001/jamaophthalmol.2017.3431> PMID:28910435
11. Rosenfeld PJ, Durbin MK, Roisman L, et al. ZEISS Angioplex™ Spectral Domain Optical Coherence Tomography Angiography: technical Aspects. *Dev Ophthalmol*. 2016;56:18-29. <https://doi.org/10.1159/000442773> PMID:27023249



12. Cheung CY, Ong YT, Hilal S, et al. Retinal ganglion cell analysis using high-definition optical coherence tomography in patients with mild cognitive impairment and Alzheimer's disease. *J Alzheimers Dis.* 2015;45(1):45-56. <https://doi.org/10.3233/JAD-141659> PMID:25428254
13. Yiu G, Pecen P, Sarin N, et al. Characterization of the choroid-scleral junction and suprachoroidal layer in healthy individuals on enhanced-depth imaging optical coherence tomography. *JAMA Ophthalmol.* 2014;132(2):174-181. <https://doi.org/10.1001/jamaophthalmol.2013.7288> PMID:24336985
14. Chandrasekera E, Wong EN, Sampson DM, Alonso-Caneiro D, Chen FK. Posterior Choroidal Stroma Reduces Accuracy of Automated Segmentation of Outer Choroidal Boundary in Swept Source Optical Coherence Tomography. *Invest Ophthalmol Vis Sci.* 2018;59(11):4404-4412. <https://doi.org/10.1167/iovs.18-24665> PMID:30193311
15. Vuong VS, Moisseiev E, Cunefare D, Farsiu S, Moshiri A, Yiu G. Repeatability of Choroidal Thickness Measurements on Enhanced Depth Imaging Optical Coherence Tomography Using Different Posterior Boundaries. *Am J Ophthalmol.* 2016;169:104-112. <https://doi.org/10.1016/j.ajo.2016.06.023> PMID:27345731
16. Yoon SP, Grewal DS, Thompson AC, et al. Retinal Microvascular and Neurodegenerative Changes in Alzheimer's Disease and Mild Cognitive Impairment Compared with Control Participants. *Ophthalmol Retina.* 2019;3(6):489-499. <https://doi.org/10.1016/j.oret.2019.02.002> PMID:31174670
17. Anegondi N, Kshirsagar A, Mochi TB, Sinha Roy A. Quantitative Comparison of Retinal Vascular Features in Optical Coherence Tomography Angiography Images From Three Different Devices. *Ophthalmic Surg Lasers Imaging Retina.* 2018;49(7):488-496. <https://doi.org/10.3928/23258160-20180628-04> PMID:30021035
18. Munk MR, Giannakaki-Zimmermann H, Berger L, et al. OCT-angiography: A qualitative and quantitative comparison of 4 OCT-A devices. *PLoS One.* 2017;12(5):e0177059. <https://doi.org/10.1371/journal.pone.0177059> PMID:28489918
19. Al-Sheikh M, Akil H, Pfau M, Sadda SR. Swept-Source OCT Angiography Imaging of the Foveal Avascular Zone and Macular Capillary Network Density in Diabetic Retinopathy. *Invest Ophthalmol Vis Sci.* 2016;57(8):3907-3913. <https://doi.org/10.1167/iovs.16-19570> PMID:27472076
20. Fujiwara A, Morizane Y, Hosokawa M, et al. Factors affecting foveal avascular zone in healthy eyes: an examination using swept-source optical coherence tomography angiography. *PLoS One.* 2017;12(11):e0188572. <https://doi.org/10.1371/journal.pone.0188572> PMID:29176837
21. Kuehlewein L, Tepelus TC, An L, Durbin MK, Srinivas S, Sadda SR. Noninvasive Visualization and Analysis of the Human Parafoveal Capillary Network Using Swept Source OCT Optical Microangiography. *Invest Ophthalmol Vis Sci.* 2015;56(6):3984-3988. <https://doi.org/10.1167/iovs.15-16510> PMID:26087363
22. Linderman R, Salmon AE, Strampe M, Russillo M, Khan J, Carroll J. Assessing the Accuracy of Foveal Avascular Zone Measurements Using Optical Coherence Tomography Angiography: segmentation and Scaling. *Transl Vis Sci Technol.* 2017;6(3):16-16. <https://doi.org/10.1167/tvst.6.3.16> PMID:28616362
23. Tan CS, Lim LW, Chow VS, et al. Optical Coherence Tomography Angiography Evaluation of the Parafoveal Vasculature and Its Relationship With Ocular Factors. *Invest Ophthalmol Vis Sci.* 2016;57(9):OCT224-OCT234. <https://doi.org/10.1167/iovs.15-18869> PMID:27409476
24. Yu J, Jiang C, Wang X, et al. Macular perfusion in healthy Chinese: an optical coherence tomography angiogram study. *Invest Ophthalmol Vis Sci.* 2015;56(5):3212-3217. <https://doi.org/10.1167/iovs.14-16270> PMID:26024105
25. Laatikainen L, Larinkari J. Capillary-free area of the fovea with advancing age. *Invest Ophthalmol Vis Sci.* 1977;16(12):1154-1157. PMID:924747
26. You QS, Chan JCH, Ng ALK, et al. Macular Vessel Density Measured With Optical Coherence Tomography Angiography and Its Associations in a Large Population-Based Study. *Invest Ophthalmol Vis Sci.* 2019;60(14):4830-4837. <https://doi.org/10.1167/iovs.19-28137> PMID:31747685
27. Gadde SG, Anegondi N, Bhanushali D, et al. Quantification of Vessel Density in Retinal Optical Coherence Tomography Angiography Images Using Local Fractal Dimension. *Invest Ophthalmol Vis Sci.* 2016;57(1):246-252. <https://doi.org/10.1167/iovs.15-18287> PMID:26803800
28. Rao HL, Pradhan ZS, Weinreb RN, et al. Determinants of Peripapillary and Macular Vessel Densities Measured by Optical Coherence Tomography Angiography in Normal Eyes. *J Glaucoma.* 2017;26(5):491-497. <https://doi.org/10.1097/IJG.0000000000000655> PMID:28263261
29. Sampson DM, Gong P, An D, et al. Axial Length Variation Impacts on Superficial Retinal Vessel Density and Foveal Avascular Zone Area Measurements Using Optical Coherence Tomography Angiography. *Invest Ophthalmol Vis Sci.* 2017;58(7):3065-3072. <https://doi.org/10.1167/iovs.17-21551> PMID:28622398
30. Lee WH, Park JH, Won Y, et al. Retinal Microvascular Change in Hypertension as measured by Optical Coherence Tomography Angiography. *Sci Rep.* 2019;9(1):156. <https://doi.org/10.1038/s41598-018-36474-1> PMID:30655557